CONF-850103—5

DE85 005020

Paper to be presented at the

Second Symposium on Space Nuclear Power Systems

to be held in

Albuquerque, New Mexico in January 1985

Physics Effects of Accidental Submersion of Space Power Reactors in Water

by

S. K. Bhattacharyya

and

R. M. Lell

Argonne National Laboratory
9700 South Cass Avenue
Argonne, Illinois 60439

Physics Effects of Accidental Submersion of Space Power Reactors in Water

S. K. Bhattacharyya and R. M. Lell
Argonne National Laboratory

I. INTRODUCTION

A major safety concern for nuclear reactors in space power applications is the effect of accidental submersion of the reactors in water. Such a situation might be postulated, for example, as a consequence of a launch pad accident. The classes of reactors proposed most frequently for use in space are fast spectrum reactors, for which submersion results in a softened core neutron spectrum caused by the displacement of the liquid metal coolant by the water. The softened spectrum alters the neutron balance in the core--neutron capture and fission are increased while leakage from the core is reduced. Water outside the submerged core introduces an increased number of reflected thermalized neutrons into the core. The net effect is a function of the specific features of the reactor design (composition, size, etc.) and can be positive or negative depending upon the contributions of the individual effects. Anlaysis of the magnitude of the effect requires an accurate evaluation of the individual components. At present a designer must rely on detailed calculations performed after key design parameters are settled to determine the effects of submersion. The purpose of our work is to develop generic features of the submersion phenomenon to provide designers a means to an a priori knowledge of the impact of potential design choices on submersion reactivity.

II. CALCULATIONAL METHODS AND MODELS

Since the submersion reactivity effect is a balance between individual competing effects, it is necessary to use rigorous methods to calculate it. Earlier work on similar problems has shown the importance of accurate neutron leakage evaluations.[1,2] For this work we have selected the Monte Carlo method as our primary analytical tool with S_n transport calculations used in a supporting role in understanding the detailed physics of the problem.

All Monte Carlo calculations were performed with the VIM Monte Carlo code.[3] VIM offers the advantages of a very flexible combinatorial geometry treatment which permits very accurate representation of complex geometrical details and a continuous energy cross section treatment which eliminates multigroup approximations. For cases where Monte Carlo statistical uncertainties might mask underlying physical effects, where pointwise flux or power distributions were desired, or where the VIM continuous energy treatment and geometrical capabilities were not required, one-dimensional S_n calculations were performed. The ONEDANT code[4] was used for all S_n calculations; the required cross sections were generated with the MC2-II code.[5] MC2-II processes ENDF data into the desired multigroup format. MC2-II does not contain a rigorous thermal cross section treatment, but this is not an important point for present purposes. This paper shows that the neutron flux at thermal energies is negligible in the configurations examined here, even under flooding conditions.

In order to study the submersion problem generically, i.e., without reference to specific design concepts, three sets of calculations were performed. Infinite lattice Monte Carlo cell calculations (reflecting boundary conditions) were used to study effects of basic core parameters (fissile enrichment, volume fractions, material compositions, etc.) on Δk_∞, the non-leakage part of the submersion reactivity change. Neutron reflection effects were studied in a set of transport (S_n) calculations in which core dimensions were varied for a specific core/reflector composition. These calculations were also used to study the problem of reactor break-up prior to submersion. Finally, submersion effects were studied for a set of core designs in the 2-50 MWt power range. These designs were specifically developed for this study with core compositions and volume fractions generally representative of current thinking and the sizes and beginning-of-life material inventories selected on the basis of detailed REBUS-3 burnup calculations.[6]

Table I presents the definitions of the three unit cells used in the lattice calculations. Cell A in Table I is the reference for all cell calculations. The dimensions and volume fractions were selected as

reasonable values for a 37-pin fuel assembly in a liquid metal-cooled reactor based upon evolving SP-100 reactor designs and extrapolations to higher power systems. They include the essential features of a space power reactor core-high burnup capability and adequate heat removal for minimum system mass. Cells B and C in Table I are perturbations on the reference cell, defined to study effects of cell size and material volume fractions.

The compositions of the liner, clad, and structure in cell A were varied to study the dependence of k and flooding worth on the choice of reactor materials; the fuel composition was unchanged throughout this sequence. Each configuration was computed with Li-7 and with water in the coolant channel. Axial leakage was permitted, but reflecting boundary conditions were imposed on the hexagonal cell boundaries in the X-Y plane. Several reasonable clad/structural materials were studied. W-Re and Mo-Re are possible alternatives to ASTAR for high power applications. Nb-Zr-C is a leading candidate for the SP-100 design and might be considered for other space applications. Stainless steel is not presently being considered for such uses, but it was included to provide a bounding case.

III. RESULTS

A. LATTICE CALCULATIONS

The results of the lattice calculations are shown in Table II. Table II clearly demonstrates the effects of different clad/structural materials on base reactivity (or required uranium enrichment) of the reactor. The differences in base k's result from differences in absorptivities of the various clad materials. More importantly for present purposes, this table shows that k decreases upon flooding for all cases studied and that the magnitude of the decrease depends strongly on the type of clad/structural material. Flooding worths for ASTAR and W-Re are nearly double those for Nb-Zr-C and stainless steel. This difference becomes relevant in actual reactors where core size effects are important.

It seems contrary to first expectations that flooding decreases k, but all of the cell calculations confirm this. The explanation of the decrease in k lies in comparison of the fission and capture cross sections in the fuel and clad/structure and in the examination of the base and flooded cell spectra. Figure 1 shows $\nu\Sigma_f$ for the UN and Σ_c for ASTAR and Nb-Zr-C. Figures 2 and 3 show neutron spectra for the ASTAR and Nb-Zr-C cases under base and flooding conditions. Flooding does cause spectral softening, but the downward shift is small because of the low coolant volume fraction and because of high absorptivity in the clad/structure. Capture cross sections of the clad/structural materials increase much more rapidly than does neutron production over most of the energy range in Fig. 1. Upon comparing cross sections in Fig. 1 with base and flooded spectra in Figs. 2 and 3, it becomes obvious that addition of water only shifts neutrons down to energies where the capture-to-fission ratio is significantly higher than in the base configuration. To obtain positive worths in the cell calculations, it would be necessary to shift neutron energies down into the low energy range before the neutrons are absorbed in the clad. This seems difficult to accomplish in realistic cell configurations.

Material volume fractions and, consequently, some cell dimensions were varied for the second set of cell calculations. The variations are shown in Table I. The fuel pin size was preserved in all cases because the fuel pin size is the constrained quantity for fixed power and burnup limits. Table III shows the results of these variations. Case B of Table III has slightly less clad/structure and significantly less coolant than case A; case C has slightly more clad/structure and significantly more coolant than case A. The flooding worth for case A falls approximately midway between the values for cases B and C. The differences in the amounts of clad/ structure present in the three cases contribute to the differences in the flooding worth. However, the major contributor to the differences is the variation in coolant volume. The decreased coolant volume in case B causes less spectral shift than in case A; the increased coolant volume in case C causes greater spectral shift than in case A. Because of the different energy dependences of the fission and clad capture cross sections, larger spectral shift leads to an increased

percentage of captures in the clad and to lower cell eigenvalues. Consequently, increasing the coolant volume causes an increase in the magnitude of flooding worth.

Two factors were varied for the last set of cell calculations. The base and flooded configurations for cell A in Table I were recomputed with uranium enrichments of 25%, 50%, and 93%; all other compositions and dimensions were as shown in the table. To test the importance of heterogeneity, these calculations were performed for heterogeneous cells (as were all cases cited above) and for equivalent homogeneous cells. Table IV and Fig. 4 show the results. Table IV demonstrates that flooding worth is negative for the entire range of enrichments studied. The shapes of the curves in Fig. 4 indicate that the magnitude of the flooding worth peaks between 60% and 65% enrichment. The location of the peak is slightly shifted toward lower enrichment for homogeneous cells, but this shift may just be a product of the Monte Carlo statistical uncertainties. Figure 4 shows a small heterogeneity effect, i.e., a small difference between heterogeneous and homogeneous cell results. This effect is small compared to the magnitudes of the reactivity changes exhibited in the cell calculations. However, the heterogeneity effect is large enough to become relevant in situations where reactivities are small or k approaches unity. The heterogeneous and homogeneous curves begin to diverge for high enrichment because parasitic capture appears to increase more rapidly under flooding conditions at very high enrichments.

B. VARIATIONS OF WORTHS WITH CORE SIZE

An asymptotic flux distribution is established in an infinite lattice; this may not be the case over much of a real reactor core. This difference complicates analysis of flooding effects in realistic configurations. The simplest transition from cell calculations to realistic core calculations is to study the influence of core radius on flooding worth for an uniform core composition. A configuration was defined based on cell A (Table I). The core was assumed to be bare i.e., no radial reflector/control drums were present, for the base case. For flooding

cases, the core was surrounded by water. The base and flooding calculations were repeated for increasing core radii. The same calculational sequence was repeated for cases in which radial reflector/control drums were present around the fuel. The B_4C segment was next to the fuel when the drums were present.

Tables V and VI and Fig. 5 show the results. Flooding worth is much higher for bare cores than for corresponding reflected cores. This accords with expectations. Water around the fuel acts as a reflector in flooded configurations. Comparison of base cases in Tables V and VI clearly demonstrates the importance of reflection. Even with B_4C next to the fuel, reflection in Table VI is a major factor in neutron economy. For both bare and reflected cores, the flooding worth is initially positive and gradually turns negative with increasing core size. For small cores, reflection on the outside is the dominant factor in determining flooding worth. Not only are neutrons which would otherwise be lost being returned to the core, but they are also being thermalized before returning to the core. This combined reflection/thermalization effect is particularly important in a small core because much of the core lies within a few optical path lengths of the core boundary and, consequently, is readily accessible to returning neutrons. For core radius R and height H in a cylindrical core, the core surface-to-volume ratio, S/V, is 2(H+R)/RH. If external drums are the principal means of reactivity control, there is strong motivation to design an elongated core to maximize drum worth. For elongated cores such as those considered here, H is much larger than R, and S/V approaches 2/R. The fraction of the core readily accessible to reflected neutrons is inversely proportional to R. As core radius increases, the fraction of the core that is not near the boundary increases, and this region tends to behave like the infinite lattice discussed above. Competition between infinite lattice behavior in the inner core and reflection/thermalization effects near the boundary determines the magnitude and sign of the flooding worth. For small radii, reflection/thermalization dominates, and flooding worth is

positive. For large radii, the infinite lattice effects dominate, and flooding worth is negative. The point at which the competing effects balance and flooding worth is zero is determined by the nature and size of actual reflector/control drums present.

ONEDANT calculations were also performed to examine the variation in flooding worth with increasing core height with a fixed 10 cm BeO axial reflector. Figure 6 shows the results. Initially, flooding worth increases sharply with increasing height, principally because the base k also increases as core height increases. However, axial reflection affects a smaller fraction of the core directly as H increases, and the base k eventually approaches an asymptotic value. This is equally true for the flooded case. As H increases, infinite lattice effects become more important than axial reflection, and the flooding worth also approaches an asymptotic value.

C. INTEGRAL STUDIES OF REASONABLE CORE DESIGNS

Because core size appears to be the dominant factor in determining the sign and magnitude of flooding worth, a range of reasonable core designs were studied. The smallest core size considered was a 2 MWt system, generally characteristic of contemporary SP-100 designs. The design used fully enriched (93%) UO_2 fuel, lithium coolant, Nb-1Zr-0.1C clad/structure and is controlled by external drums containing B_4C segments in beryllium blocks. To study larger cores, five configurations ranging from 5 MWt to 50 MWt were designed using the REBUS-3 code with the multigroup cross sections generated for the ONEDANT calculations. Each core was constructed from 37-pin assemblies based on dimensions, volume fractions, and materials for cell A in Table I. The cores consisted of 3-5 hexagonal rings (19-61 assemblies) of assemblies, depending on power level. Uranium enrichments were varied by ring to obtain uniform core power and burnup distributions with a burnup limit constraint.

For each of the five cores, ONEDANT calculations were performed for the base and flooded configurations with B_4C control segments rotated

inside next to the fuel. To provide reference eigenvalues and to check the importance of the multigroup cross section approximation, these configurations were recomputed with VIM. ONEDANT calculations were also performed for base and flooded configurations with the radial reflector/control drums lost, i.e., bare core configurations. Table VII shows the results. Comparison of the Monte Carlo and corresponding S_n results shows that the two sets of calculations agree reasonably well. There are small differences in eigenvalues and worths (beyond the level of statistical uncertainty), but these differences do not obscure the fact that general trends regarding eigenvalue and worth changes between various configurations are consistent in direction and magnitude for the Monte Carlo and S_n calculations. The observed differences are consistent with differences between multigroup and continuous energy cross section treatments and with the level of statistical uncertainty achieved in the Monte Carlo calculations. This general agreement supports the use of multigroup S_n calculations here.

Flooding worth decreases (becomes less positive or more negative) as core size increases radially or axially. For cores with identical radii, e.g., cores 2 and 3 or cores 4 and 5, the longer core has smaller flooding worth because of the core height effect discussed above. As core height increases, the fraction of the core isolated from direct effects of axial reflection increases, and this portion of the core tends to behave like an infinite lattice. Consequently, as core height increases, an increasing fraction of the core makes a negative contribution to the flooding worth. In realistic configurations, this matter is complicated by variations in fuel compositions and core size introduced in designing optimal reactors subject to varying operational requirements and constraints. Nevertheless, it appears that axial reflection effects and the change in axial reflection after flooding are principally responsible for the decrease in flooding worth as core height increases.

Despite differences in fuel composition and core height, flooding worth decreases as core radius increases, even for cores with the same power level, e.g., cores 3 and 4 or cores 5 and 6. Previous results have shown that flooding worth becomes more negative as core radius increases

for uniform fuel composition. The cell calculations in Table IV show that changes in uranium enrichment do not strongly affect the sign or magnitude of flooding worth. Changes in core height do affect flooding worth but not as strongly as do changes in radius. For elongated cores such as those considered here, H is much larger than R, so S/V approaches 2/R. In other words, the top and bottom core surface areas are much smaller than the radial surface area, and axial reflection effects are much less important than radial effects. For a shortened core in which core height and diameter are nearly equal, this approximation breaks down. However, for most configurations considered here, H is much larger than R, and radial reflection effects dominate over axial reflection effects. It seems clear that flooding worth decreases with increasing core radius, even when the cores in question have different uranium enrichments and heights, as long as core height is significantly greater than core radius.

The effect of radial reflector/control drum loss on flooding worth for realistic cores is consistent with values computed for unreflected cores of uniform composition discussed above. The magnitudes of the worths for different core sizes are similar to those shown in Table V. Worths in Table VII are not identical to those in Table V because fuel grading increases the U-235 concentration from ring to ring as the radius increases, and the increased U-235 concentration emphasizes the outer fuel rings and the importance of radial reflection. Consequently, the magnitude of flooding worth is slightly larger for unreflected graded cores than it is for unreflected uniform cores of similar radii. Further, the magnitude of flooding worth is much larger in unreflected cores than in corresponding reflected cores.

IV. RELEVANT TERRESTRIAL EXPERIMENTAL EVIDENCE

In addition to the well documented SNAP work, there are experimental and concurrent analytical data obtained during the fast breeder reactor development program that are relevant to the space reactor submersion and compaction problem. The problem of steam entry in a gas cooled fast

reactor has been studied extensively at various laboratories around the world. A very detailed critical experimental program was undertaken at Argonne National Laboratory in which solid polyethylene foam strips were used as a steam simulant.[1] The program simulated the entry of various densities of steam in the GCFR core and for each configuration detailed neutronic measurements were made. These measurements included:

- Neutron spectra using proton-recoil spectrometers
- Reaction rates at various spatial locations
- Reactivity worths of materials
- Control worths
- Safety coefficients

Detailed calculations were performed of the experiments using design methods and also Monte Carlo codes. It was seen from comparison of the calculations against the experiment that the low-energy component of the flux was miscalculated by standard design methods. This led to small discrepancies in individual reaction rates, but the effect on the net steam entry worth was large since the worth was the sum of two nearly equal components of opposite sign. For the critical experiments even the sign of the steam entry worth was mispredicted by design methods. The misprediction was corrected by applying more rigorous procedures to the entire analytical package.

While the degree of spectral softening for the space reactor submersion problem is smaller than that for the GCFR steam entry problem, the lesson to be learned from the earlier studies is that critical experiments should be used to calibrate calculational methods used for submersion analyses to gain confidence in the computed submersion worths.

A major experimental and analytical study of distorted LMFBR reactor cores was performed at ANL in 1977.[2] A number of compacted and voiding core configurations were simulated in a critical assembly and a detailed neutronic characterization was made of each configuration. The reactivity worths of compaction and voiding were determined and compared to calculations. It was found that standard design methods grossly mispredicted these worths and the mispredictions were in a non-conservative direction. Monte Carlo methods give much better agreement, but there were significant discrepancies compared to experiment.

Compaction scenarios for the space reactors have not been established yet. However, based on the earlier results it is clear that critical experimental verification/calibration of methods will be essential to gaining confidence in the analytical studies of these accident conditions.

V. SUMMARY

Several general tendencies can be established from the lattice cell calculations cited in Section III. In an infinite lattice, the flooding worth is negative for all clad/structural materials studied. For the materials considered (which include most of the leading candidate materials) and reasonable cell dimensions, flooding causes a spectral shift down into an energy range where the ratio of parasitic capture to neutron production cross sections increases with decreasing energy.

The size of the flooding effect depends on core volume fractions, particularly coolant volume fraction. As the coolant volume fraction increases, the magnitude of the worth increases while the sign of the worth remains negative. For very large coolant volume fractions (well beyond those presently considered reasonable for practical designs), considerable spectral softening occurs, and deviations from the monotonic cross section pattern appear which could lead to positive worths.

The cell calculations showed a small dependence of flooding worth on fuel enrichment with a peak around 60-65% enrichment. They also

showed a very small heterogeneity effect, i.e., a difference in computed worth between heterogeneous and homogeneous cell calculations.

Calculations showed that core size is a major determinant of the sign and magnitude of flooding worth. Studies established that the magnitude of flooding worth is much larger for a bare core, e.g., one in which the reflector/control drums have broken off prior to submersion, than in a reflected core of the same core fuel radius. For both reflected and unreflected cores, the net effect of submersion is positive for small core sizes and goes negative as core radius increases. For reflected cores, the positive worth is smaller and the crossover point occurs at smaller core radius. The cause of this behavior is competition between infinite lattice behavior near the core center and reflection/thermalization near the core boundary. The interplay of these two factors determines the sign and magnitude of the flooding worth in a given case. Calculations for more practical, i.e., less idealized, core designs confirm these results.

Spectrum softening and core distortion effects have been studied earlier for terrestrial fast reactor applications. These experimental and analytical studies revealed difficulties in accurately analyzing effects of spectral softening and core distortion, e.g., core compaction, and demonstrated the need for critical experiments to benchmark and calibrate analytical methods for space reactor design. Until critical experiments are performed, generic analyses based on S_n and Monte Carlo methods can be used to assess key features of flooding and core distortion phenomena and to study the interplay of individual components of these phenomena in realistic reactor configurations.

REFERENCES

1. S. K. Bhattacharyya, et. al., "The Effect of Accidental Steam Entry on GCFR Integral Neutronics Parameters," Nucl. Tech. Vol. 50, pp 197-218, October 1980.

2. S. K. Bhattacharyya, et. al., "A Critical Experimental Study of Integral Physics Parameters in Simulated LMFBR Meltdown Cores," Nucl. Tech., Vol. 46, No. 3, pp 517-524, December 1979.

3. R. N. Blomquist, et. al., "VIM - A Continuous Energy Monte Carlo Code at ANL," ORNL/RSIC-44, pp 31-46, August 1980.

4. R. D. O'Dell, et. al., "User's Manual for ONEDANT: A Code Package for One-Dimensional, Diffusion-Accelerated, Neutral-Particle Transport," Los Alamos National Laboratory, LA-9184-M, February 1982.

5. H. Henryson, II, et. al., "MC^2-2: A Code to Calculate Fast Neutron Spectra and Multigroup Cross Sections," Argonne National Laboratory, ANL-8144 (ENDF 239), June 1976.

6. B. J. Toppel, "A User's Guide for the REBUS-3 Fuel Cycle Analysis Capability," Argonne National Laboratory, ANL-83-2, March 1983.

Table I. Parameters of Reference Cell Used in Calculations

Cell	A	B	C
Dimensions, cm			
Liner ID	0.88	0.88	0.88
Clad ID	0.90	0.90	0.89
Clad OD	1.02	1.06	1.00
Cell Pitch	1.18	1.32	1.08
Fuel Length	150.0	150.0	150.0
Axial Reflector Length	10.0	10.0	10.0
Volume Fractions			
Fuel	0.50	0.40	0.60
Liner	0.02	0.02	0.02
Clad	0.16	0.16	0.16
Structure	0.07	0.07	0.07
Coolant	0.25	0.35	0.15
Materials			
Fuel	UN	UN	UN
Liner	W	W	W
Clad	ASTAR	ASTAR	ASTAR
Structure	ASTAR	ASTAR	ASTAR
Coolant	Li-7	Li-7	Li-7
U Enrichment	93%	93%	93%

Table II. Lattice k_∞ as a Function of Liner and Clad/Structure Materials for Reference Cell A

Case	Liner	Clad/ Structure	k, Base	k, Flooded	Δk, F-B
1	W	ASTAR	1.776 ±0.005	1.452 ±0.004	-0.324 ±0.006
2	W	W-24Re	1.823 ±0.004	1.511 ±0.004	-0.312 ±0.006
3	W	Nb-1Zr-.1C	1.929 ±0.003	1.726 ±0.005	-0.203 ±0.006
4	W	SS316	1.975 ±0.003	1.796 ±0.003	-0.179 ±0.004
5	W	Mo-14Re	1.902 ±0.004	1.646 ±0.004	-0.256 ±0.005
6	Nb-1Zr-.1C	Nb-1Zr-.1C	1.932 ±0.003	1.758 ±0.005	-0.174 ±0.006
7	SS316	SS316	1.992 ±0.003	1.827 ±0.003	-0.165 ±0.004
8	Mo-14Re	Mo-14Re	1.907 ±0.004	1.651 ±0.004	-0.256 ±0.006

Table III. Effects of Cell Dimensions and Volume Fractions on Flooding Worth

Cell	k, Base	k, Flooded	Δ k, F-B
A	1.776 ± 0.005	1.452 ± 0.004	-0.324 ± 0.006
B	1.702 ± 0.004	1.284 ± 0.005	-0.418 ± 0.007
C	1.836 ± 0.005	1.624 ± 0.006	-0.212 ± 0.008

Table IV. Effects of Cell Heterogeneity and Uranium Enrichment on Flooding Worth in Reference Cell

Enrichment	Heterogeneous Cell k	Homogeneous Cell k	Δ k, Het. - Hom
93%			
k, Base	1.776 ± 0.005	1.779 ± 0.003	-0.003 ± 0.006
k, Flooded	1.452 ± 0.004	1.481 ± 0.003	-0.029 ± 0.005
Δk, F-B	-0.324 ± 0.006	-0.298 ± 0.004	---------
50%			
k, Base	1.449 ± 0.005	1.448 ± 0.003	0.001 ± 0.006
k, Flooded	1.118 ± 0.004	1.125 ± 0.004	-0.007 ± 0.006
Δk, F-B	-0.331 ± 0.006	-0.323 ± 0.005	---------
25%			
k, Base	1.046 ± 0.004	1.040 ± 0.002	0.006 ± 0.005
k, Flooded	0.798 ± 0.005	0.802 ± 0.005	-0.004 ± 0.007
Δk, F-B	-0.247 ± 0.006	-0.238 ± 0.005	---------

Table V. Effects of Core Radius on k and Flooding Worth for Unreflected (Bare) Cores-Uranium Enrichment 50%

Core Radius, cm	k, Base[a]	k, Flooded[b]	Δk, F-B
3.78	0.143	0.541	0.398
6.89	0.271	0.706	0.435
10.00	0.405	0.806	0.401
16.48	0.670	0.928	0.258
22.99	0.877	0.995	0.118
29.52	1.024	1.037	0.013
36.06	1.127	1.063	-0.064

a) For base configurations, core was bare, i.e., no reflection present.

b) For flooded configurations, a 75 cm water reflector surrounded the fuel.

Table VI. Effects of Core Radius on k and Flooding Worth for Core with Reflector/Control Drums (B_4C Turned In)-Uranium Enrichment 50%

Core Radius, cm	k, Base	k, Flooded[a]	Δk, F-B
3.78	0.207	0.237	0.030
10.00	0.534	0.614	0.080
16.48	0.787	0.824	0.037
22.99	0.965	0.936	-0.029
29.52	1.086	1.000	-0.086
36.06	1.170	1.040	-0.130

a) For flooded configurations, 75 cm of water surrounded the control drums.

Table VII. Flooding Reactivity Worths for Representive Core Configurations

Reference Core	1	2	3	4	5	6
Power (MWt)	2	5	10	10	50	50
Core Radius, cm	15.62	16.48	16.48	22.99	22.99	29.52
No of Radial Fuel Zones	1	3	3	4	4	5
H/D	0.96	1.40	2.73	1.02	4.96	2.21
S_n Reflected Core, B_4C Inside						
k, Base		0.888	0.872	0.952	0.931	0.984
k, Flooded		0.937	0.902	0.959	0.893	0.903
Δk, F-B		0.049	0.030	0.007	-0.037	-0.081
Unreflected Core,						
k, Base			0.734		0.833	0.915
k, Flooded		1.066	1.030	1.039	0.971	0.960
Δk, F-B			0.296		0.138	0.045
Monte Carlo Reflected Core, B_4C Inside						
k, Base	0.867 ±0.005	0.883 ±0.004	0.858 ±0.005	0.942 ±0.004	0.926 ±0.004	0.985 ±0.004
k, Flooded	0.995 ±0.006	0.916 ±0.005	0.889 ±0.004	0.941 ±0.004	0.881 ±0.003	0.902 ±0.004
Δk, F-B	0.128 ±0.008	0.033 ±0.006	0.031 ±0.006	-0.001 ±0.006	-0.045 ±0.005	-0.083 ±0.006

Table VIII. Comparison of Calculated Flooding Reactivity Worths for Representative Core Configurations

Reference Core	Δk (Monte Carlo)	Δk (Transport Theory)
° 2 MWt	0.128 ± 0.008	
° 5 MWt (Case 2)	0.033 ± 0.006	0.049
° 10 MWt (Case 3)	0.031 ± 0.006	0.030
° 10 MWt (Case 4)	-0.001 ± 0.006	0.007
° 50 MWt (Case 5)	-0.045 ± 0.005	-0.038
° 50 MWt (Case 6)	-0.083 ± 0.006	-0.081

Fig. 1 Variation of macroscopic neutron production and capture cross sections of representative materials as a function of neutron energy

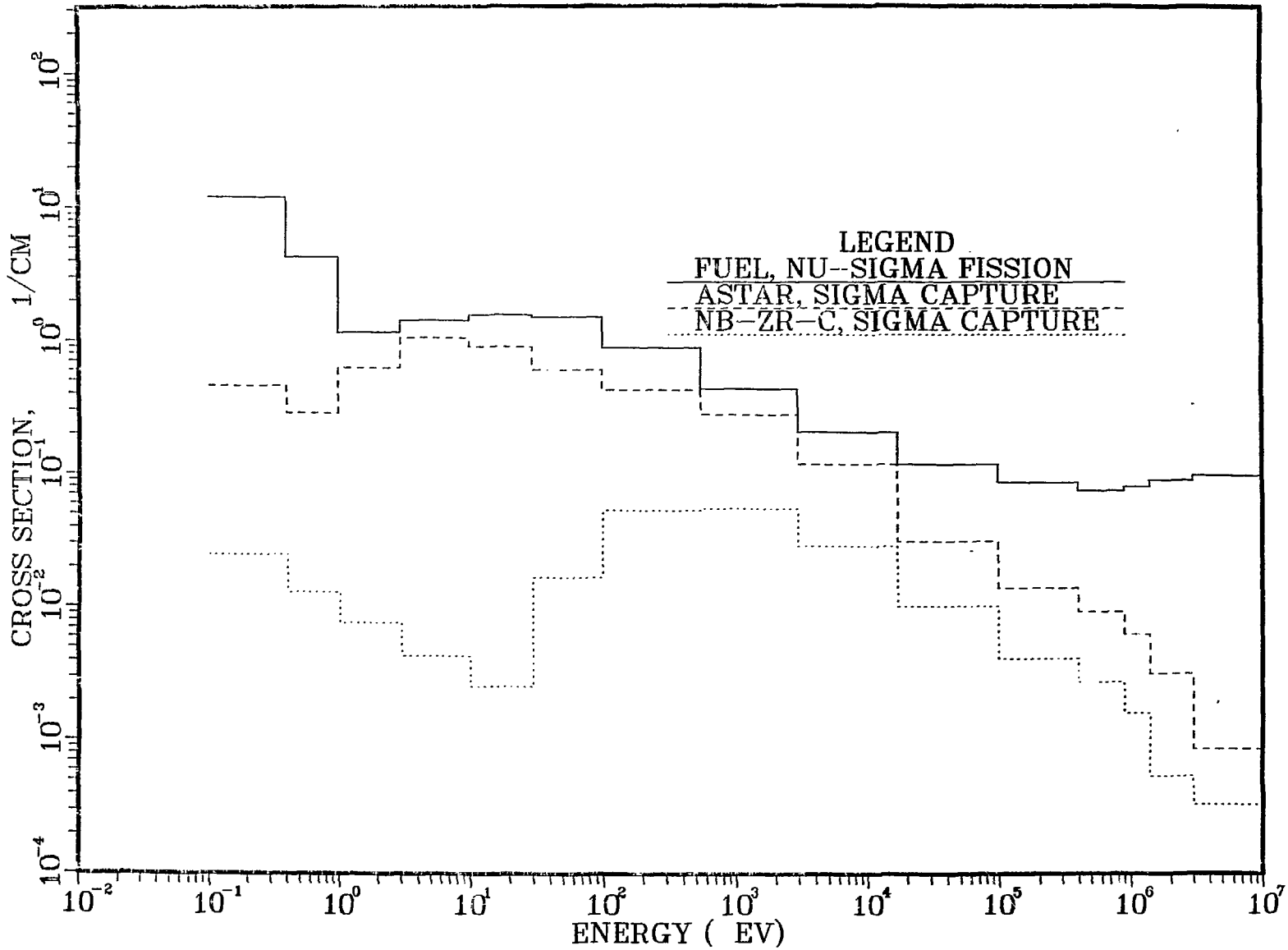

Fig. 2 Comparative neutron energy spectra for Cell A with ASTAR 811C clad-base and flooded configurations

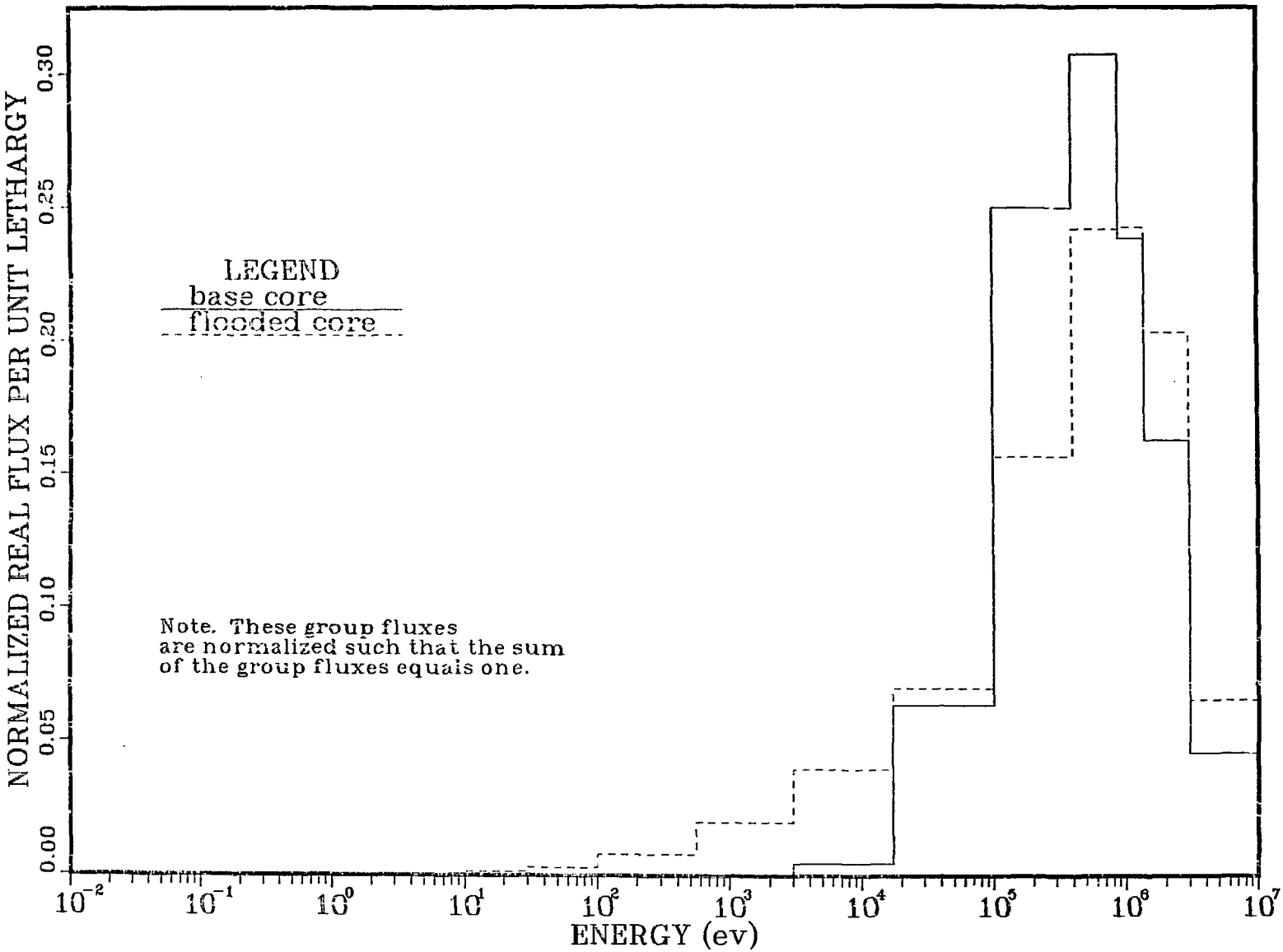

Fig. 3 Comparative neutron energy spectra for Cell A with Nb-1Zr-.1C clad-base and flooded configurations

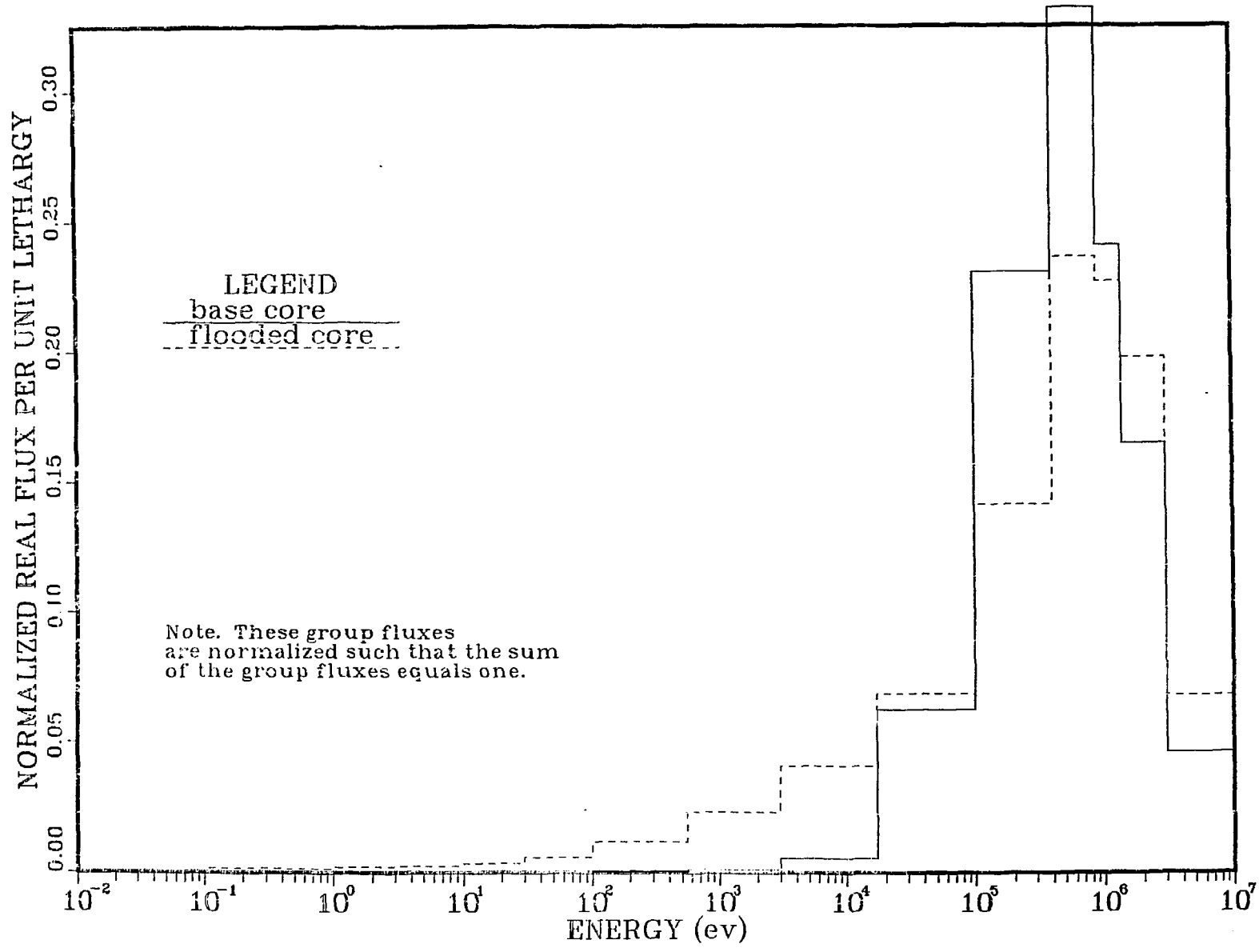

Fig. 4 Normalized submersion reactivity worth as a function of fissile enrichment and cell heterogeneity

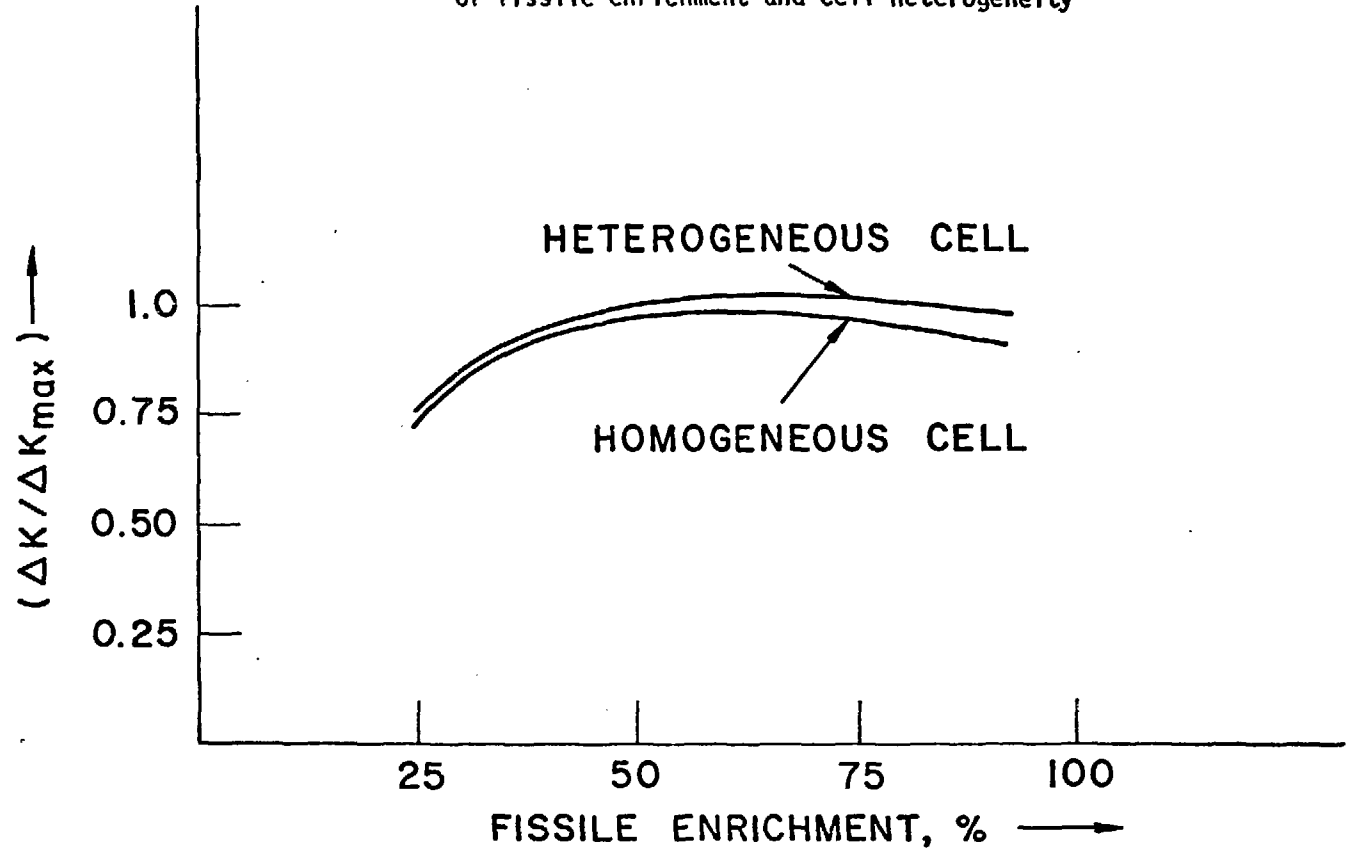

Fig. 5 Normalized submersion reactivity worth as a function of core radius for a representative ASTAR 811C clad, UN fueled reactor

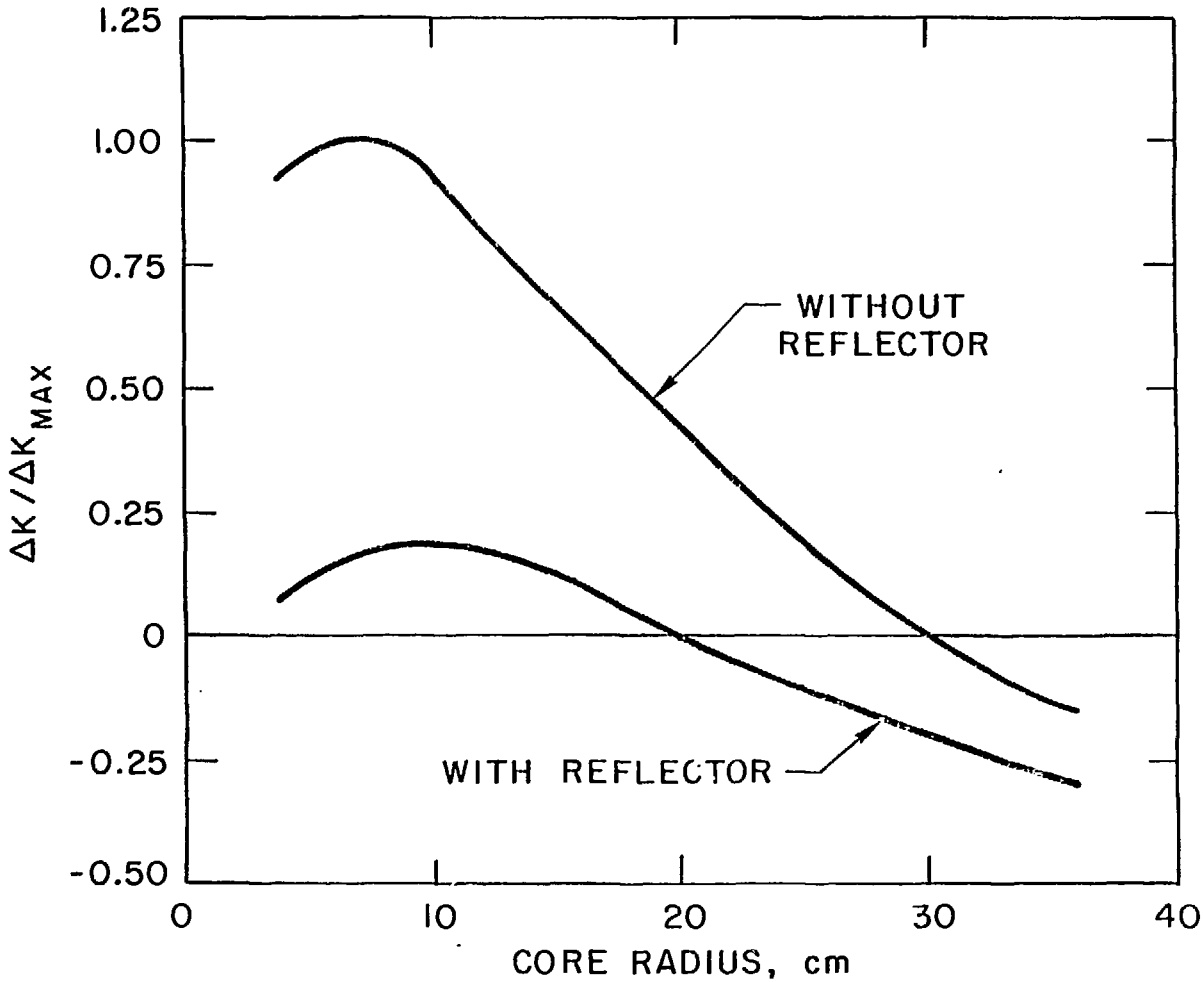

Fig. 6 Normalized submersion reactivity worth as a function of core height for infinite core radius